MEDICINE UPDATES JOURNAL
Faculty of Medicine Port Said University
Volum: 19 No:4 PP:55 - 70

"Is it Possible to Use Diffusion weighted MRI to Distinguish and Discriminate between Pathological Subtypes of Benign and Malignant Thyroid Nodules? "

Authors

Waleed Said Abo Shanab [1], Mohamed Elrakhawy [2], Carmen Ali Zarad [1], Amr Abo elfarh [3] Khaled Abd El-Baky Ahmed [1]

[1] Diagnostic Radiology, Faculty of Medicine- Port Said University
[2] Diagnostic Radiology, Faculty of Medicine - Mansoura University
[3] Radiology Department, Suez Canal Authority, Port Said

Submitted: 12/07/2024
Accepted:10/08/2024

DOI: 10.21608/muj.2024.303633.1176

ISSN : 2682-2741

https://muj.journals.ekb.egdean@med.psu.edu.eg
vice_dean_postgraduate@med.psu.edu.eg

ABSTRACT:

Background: Fine needle aspiration cytology (FNAC) is an accurate technique for diagnosing thyroid nodules. However, 10% are non-diagnostic. As a result, there is a .need for an alternative diagnostic technique

Water molecular motion in lesions and healthy tissues can be quantitatively measured with the help of diffusion-weighted imaging (DWI). The net diffusion of the water molecules is expressed in terms of the apparent diffusion coefficient .((ADC

:Aim of the study

Our goal was to evaluate the usefulness of ADC values in differentiating malignant from benign thyroid nodules, as well as pathological subtypes of each .group with FNAC correlation

:Materials and methods

Seventy patients with 70 thyroid nodules were included in this prospective study done during the period between January 2022 and March 2024. Each patient's thyroid gland nodules were examined by diffusion-weighted imaging and then intended to

Results:

The mean ADC value for the benign group is higher than for malignant nodules. The mean ADC at b = 1000 was 1.02 ± 0.381 in benign lesions, but in malignant lesions, it was 0.73 ± 0.323 with a statistically significant difference between P<0.001.

We observed a considerable overlapping in ADC values of different pathological subtypes within each group of either malignant or benign nodules with a statistically insignificant difference (P value ranged from 0.056 to 0.063).

Conclusions:

ADC values can be used to discriminate benign from malignant thyroid nodules; however, it is not possible to distinguish between several histological subtypes of each group.

Keywords:

Apparent diffusion coefficient value, Diffusion MRI, Fine needle aspiration cytology, Thyroid nodules.

Background

It is essential to differentiate between benign and malignant nodules. In patients with benign nodules, it helps to avoid unnecessary surgery. Early detection of malignant nodules lowers disease mortality and morbidity rates. [1, 2]

The assessment of non-diagnostic and inadequate samples remains an issue, and there is no widely acknowledged strategy to follow up on non-diagnostic thyroid fine needle aspiration cytology (FNAC). [3]

Diffusion-weighted MRI Imaging (DWI) detects changes in tissue microstructure that affect water diffusion. The apparent diffusion coefficient value (ADC), which is significantly lower in malignant nodules than in benign nodules, can aid in the differentiation between two types of nodules. Using a high b value, you can improve diagnostic accuracy. [4, 5]

The ideal b value for a thyroid MRI and the corresponding suggested cut-off point for ADC value to detect a malignant nodule are still debated. [6]

Aim of work:

Determining the right treatment plan for thyroid nodules requires discrimination between benign and malignant groups. Our objective was to evaluate the application of apparent diffusion coefficient values in the application of diffusion magnetic resonance imaging to distinguish between malignant and benign thyroid nodules, as well as pathological subtypes within each group.

Materials and Methods

Patients:

The time frame for this prospective study was January 2022–March 2024. It included 70 patients (43 females and 27 males) with 70 thyroid nodules. Their mean age was 46.90±11.43 years, ranging from 20 to 70 years. Before being referred for MRI examination, each patient's thyroid gland nodules were examined via ultrasonography (US). It was intended for every patient to have FNAC.

Before participating in the study, each participant signed an informed consent form that our local committee on research and ethics had authorized (ERN: MED (1/3/2022) s. no (38) RAD922_002).

Inclusion criteria:

- Patients with thyroid nodules (solitary or multiple nodules, either solid or complex nodules). In a patient showing multiple thyroid nodules, we selected the most significant nodule that showed a higher TIRADS level.
- Post-operative thyroidectomy with local recurrent masses.

Exclusion criteria:

- Pure thyroid cystic lesions.
- Diffuse thyroid diseases.
- Thyroid abscess.
- Patients contraindicated for MRI (e.g., pacemakers).
- Patients who are ineligible for aspiration (e.g., Bleeding disorders).
- Claustrophobic patients.

MRI imaging:

- Using a 1.5-T system (SIGNA™ Explorer 1.5T GE Healthcare United States of America and Achieva Philips Medical Systems, Philips Electronics MRI machines United States of America).
- Circularly polarized surface coil was placed over the neck.
- The conventional MRI protocol consisted of the following sequences:

  - Axial T1-weighted sequence with a repetition time (TR) / echo time (TE) (500/15 ms).

  - Axial and coronal spin-echo T2-weighted sequence with TR/TE (4000/90 ms).

  - The Field of view of 25 cm, with a slice thickness of 5 mm, an intersection gap of 1 mm, and an acquisition matrix of 256 × 256.

- Diffusion-Weighted MR Imaging (DWI):

  -The imaging protocol is an axial sequence, multi-section, multi-shot echo-planar imaging (EPI).

- 192 x 144 acquisition matrix; thickness of 5 mm; interslice gap of 1 mm; FOV of 25 cm; high TR of 1700 ms; short TE of 100 ms. About 1 minute and 45 seconds was the acquisition time.

- A circular ROI, measuring between 10 and 30 mm^2 depending on the size of the nodule, was selected in the center of solid nodules or on the solid section of mixed solid-cystic thyroid nodules while avoiding cystic degeneration, hemorrhage, and necrosis as much as possible.

-The system's software automatically determined the mean ADC values when ROIs were determined.

-ADC value was determined using b values of 500 and 1000 s/mm^2. Square millimeters per second (mm^2/s) express the ADC values.

-To determine the study's conclusions, comparisons of the pathological subtypes of malignant and benign nodules, as well as their lowest, maximum, and mean ADC values, were made.

- After MRI exams, FNAC and pathological evaluation were performed on every patient under US guidance.

Statistical analysis:

- After revision, coding, tabulation, and introduction to a PC, the gathered data was processed through the Statistical Package for Social Science (SPSS version 22).
- Depending on the data distribution, quantitative variables are expressed as mean. Frequencies and percentages were used to express qualitative characteristics.
- Using the Student t-test, two study groups were compared on a continuous variable. The association between the categorical variables will be investigated using the chi-square test. Regarding P-values less than 0.05, the results were considered statistically significant.
- Sensitivity, specificity, predictive value, and accuracy of the apparent diffusion coefficient values compared to the result of Ultrasound-guided FNAC of the thyroid nodules will be calculated.

Results

Seventy patients with 70 thyroid nodules were selected in this prospective study and underwent MRI with pathological examination by FNAC under ultrasound guidance.

In our study, 41 (58.6%) patients had benign thyroid nodules, which included 8 (11.4%) patients with lymphocytic thyroiditis, 12 (17.1%) patients with colloid nodules, and 21 (30%) patients with follicular adenomas. In contrast, 29 (41.4%) patients had malignant thyroid nodules, which included 2 (2.9%) patients with B-cell lymphoma, 2 (2.9%) patients with medullary carcinoma, 7 (10%) patients with follicular carcinoma, 4 (5.7%) patients with papillary carcinoma on top of follicular adenoma, and 14 (20%) patients with papillary carcinoma (Tables 1 and 2).

Table (1): pathological subtypes of benign nodules in participating subjects.

Tumor type	N	%
Lymphocytic thyroiditis	8	11.4%
Colloid nodule	12	17.1%
Follicular adenomas	21	30%
Total	41	58.6%

Table (2): pathological subtypes of malignant nodules in participating subjects.

Tumor type	N	%
B-cell lymphoma	2	2.9%
Medullary carcinoma	2	2.9%
Papillary carcinoma on top of follicular adenoma	4	5.7%
Follicular carcinoma	7	10%
Papillary carcinoma	14	20%
Total	29	41.4%

The link between ADC values and several pathological subtypes of thyroid nodules across the entire sample was described. The ADC ranged from 0.21-2.60 for the patients we investigated. Most of them, 68.6% had an ADC ≥1, and 31.4% had an ADC <1 (Table 3).

Table (3): Correlation between ADC values and various histopathological variations of thyroid nodules over the entire sample.

Variant	ADC	
	≥ 1	< 1
Lymphocytic thyroiditis	8	
Colloid nodule	10	2
Follicular adenoma	17	4
B-cell lymphoma		2
Medullary carcinoma		2
Papillary carcinoma on top of follicular adenoma	2	2
Follicular carcinoma	4	3
Papillary carcinoma	7	7
Total	48	22

The mean ADC value for the benign group was higher than for malignant nodules. The mean ADC at b = 1000 was 1.02 ± 0.381 in benign lesions, but in malignant lesions, it was 0.73 ± 0.323 with a statistically significant difference in between with P<0.001(Table 4).

Table (4): Comparison between the studied benign and malignant groups according to ADC at b = 1000.

	Benign (n = 41)	**Malignant (n =29)**	**T**	**p**
ADC				
Range	0.66 – 2.60	0.21 – 1.3	4.775*	<0.001*
Mean ± SD.	**1.02**± 0.381	**0.73**± 0.323		

t, p: t, and p values for **Student t-test** for comparing between the two groups
*: Statistically significant at p ≤ 0.05.

The lymphocytic thyroiditis's (Fig. 1) ADC value varied between 1.31 and 2.60 × 10^{-3} mm^2/s. The ADC for colloid cysts (Fig. 2) and follicular adenomas (Fig. 3) ranged from 1.0 to 2.5 × 10^{-3} mm^2/s and 0.66 to 2.37 × 10^{-3} mm^2/s, respectively. ADC values were as follows: 0.21 – 0.96 × 10^{-3} mm^2/s for follicular carcinoma (Fig. 4); 0.51 – 1.0 × 10^{-3} mm^2/s for B-cell lymphoma (Fig. 5); 0.22 – 1.30 × 10^{-3} mm^2/s for papillary carcinoma on top of follicular

adenoma; 0.67 – 0.73 × 10^{-3} mm^2/s for medullary carcinoma; and 0.20 – 0.96 × 10^{-3} mm^2/s for papillary carcinoma (Fig. 6) (Table 5).

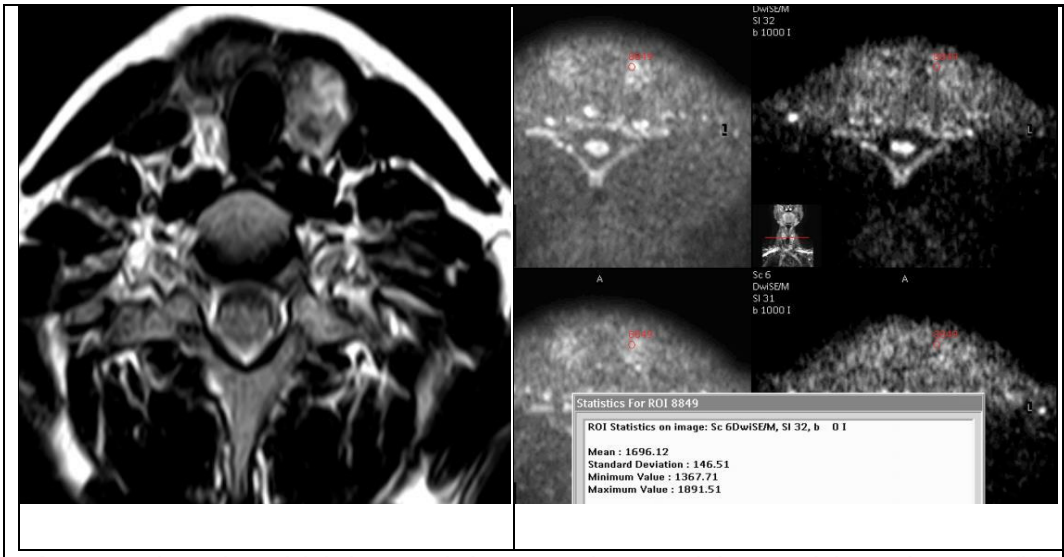

Fig. 1 A left thyroid lobe nodule was detected in T2 (a) and ADC (b) images; the ADC value was 1.69 × 10^{-3}. Lymphocytic thyroiditis was the pathology of this lesion.

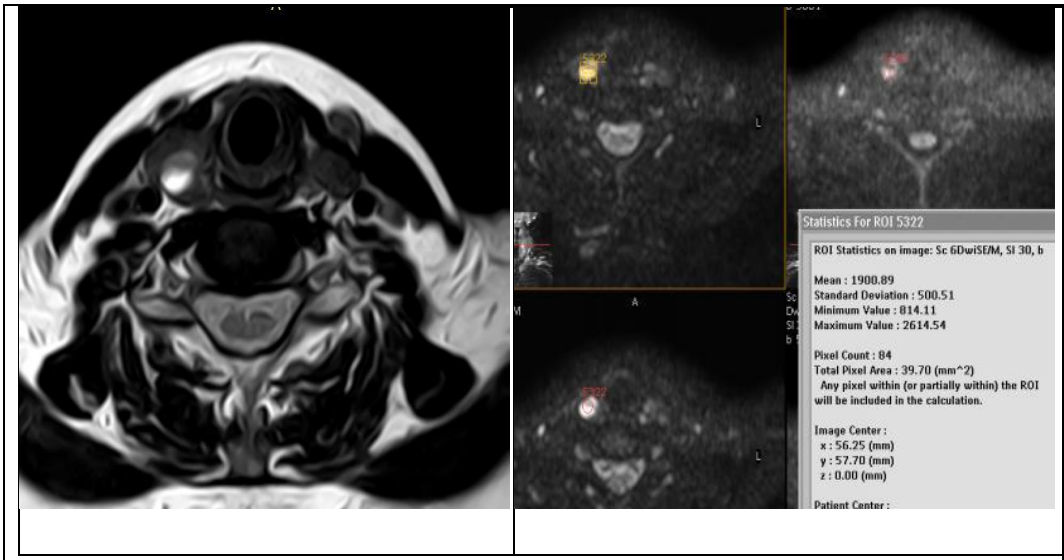

Fig. 2 The right thyroid lobe nodule was seen in T2 image (a) and ADC (b); the ADC value was around 1.9 × 10^{-3}. A colloid cyst was the pathology of this lesion.

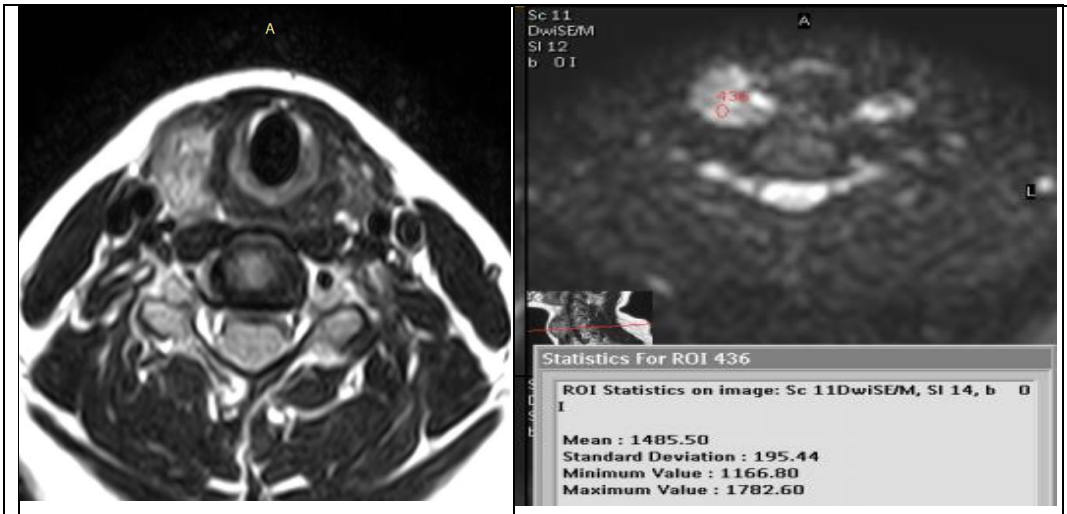

Fig. 3 The right thyroid lobe nodule appeared in T2 (a) and ADC (b) images showing that the ADC value was 1.48×10^{-3}. Follicular adenoma was the pathology of this lesion.

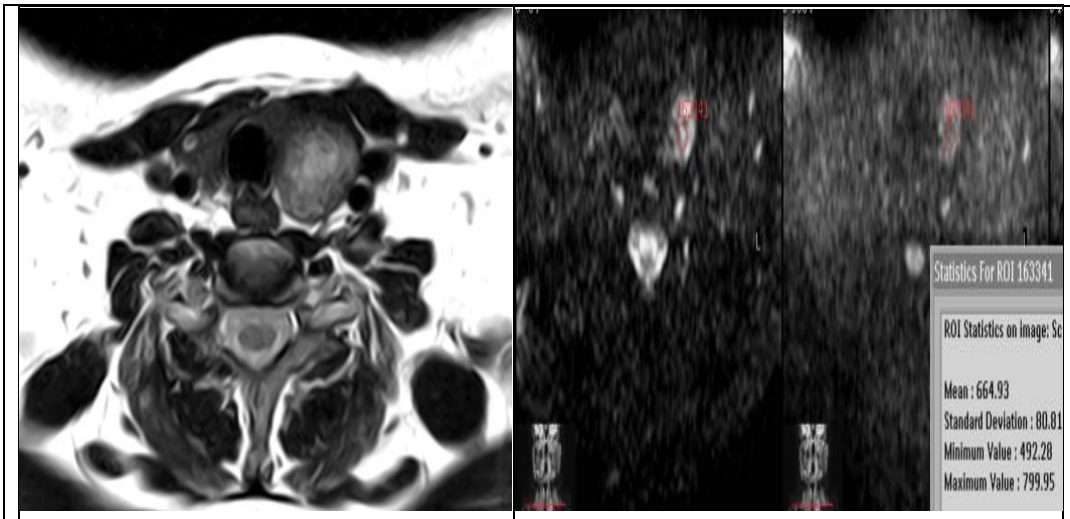

Fig. 4 A left thyroid lobe nodule is detected in T2 (a) and ADC (b) images; the ADC value was 0.66×10^{-3}. Follicular carcinoma was the pathology of this lesion.

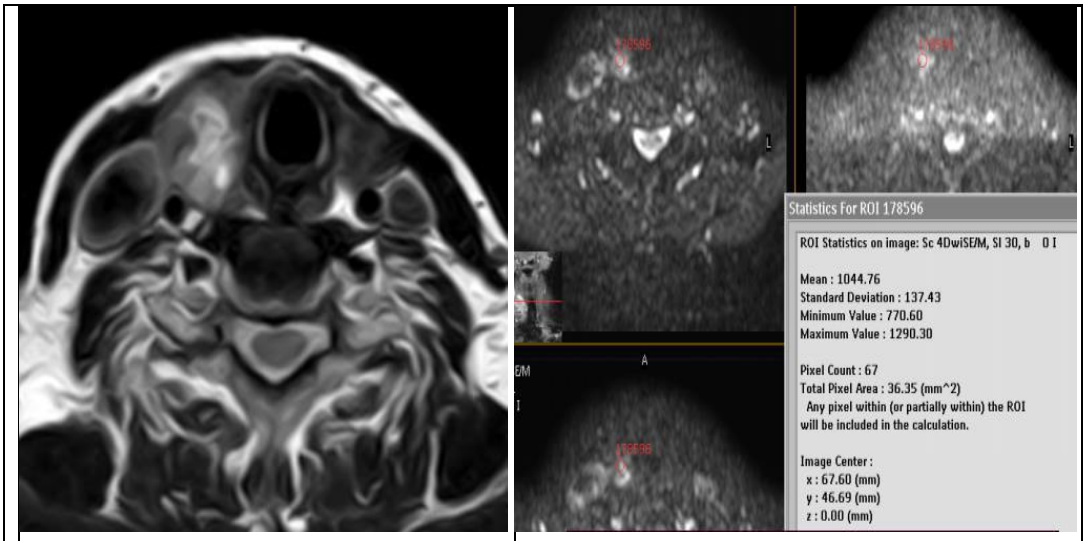

Fig. 5 A right thyroid lobe nodule is detected in T2 (a) and ADC (b) images; the ADC value was 1.0×10^{-3}. B cell lymphoma was the pathology of this lesion.

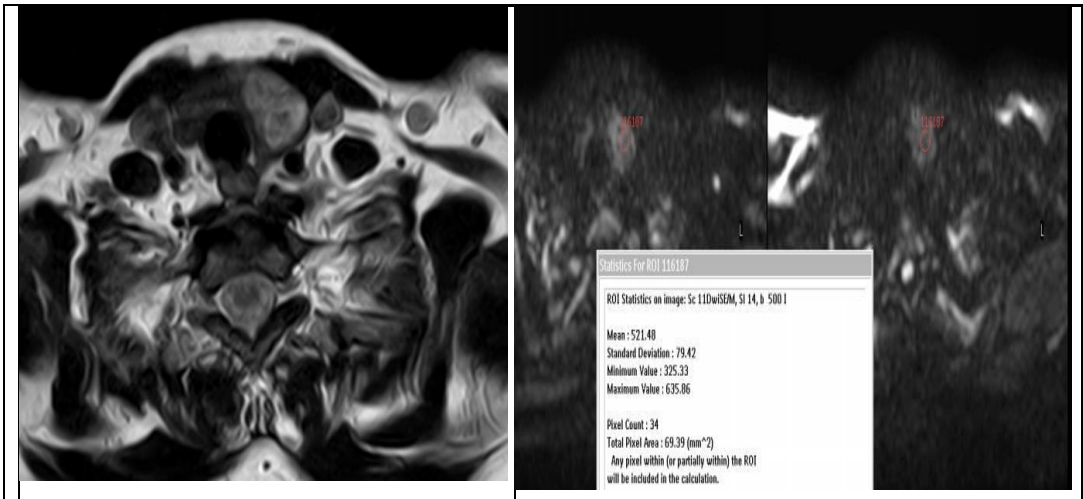

Fig. 6 A left lobe thyroid nodule was seen in T2 (a) and ADC (b) images; the ADC value was 0.52×10^{-3}. Papillary carcinoma was the nodule's pathology.

Table (5): ADC values for pathological subtypes

Type	ADC range (mm^2/s)	ADC mean (mm^2/s)
Lymphocytic thyroiditis	$1.31–2.60 \times 10^{-3}$	1.95×10^{-3}
Colloid nodule	$1.0–2.5 \times 10^{-3}$	1.75×10^{-3}
Follicular adenoma	$0.66 – 2.37 \times 10^{-3}$	1.53×10^{-3}
B-cell lymphoma	$0.51 – 1.0 \times 10^{-3}$	0.750×10^{-3}
Medullary carcinoma	$0.67 – 0.73 \times 10^{-3}$	0.70×10^{-3}
Papillary carcinoma on top of follicular adenoma	$0.22 – 1.30 \times 10^{-3}$	0.74×10^{-3}
Follicular carcinoma	$0.21 – 0.96 \times 10^{-3}$	0.57×10^{-3}
Papillary carcinoma	$0.20 – 0.96 \times 10^{-3}$	0.55×10^{-3}

When we analyzed the FNAC results, we observed that the ADC values of pathological subtypes within each group, either benign or malignant, exhibited considerable overlapping, and the range of P value was from 0.056 to 0.063, denoting statistically insignificant differences (Fig. 7).

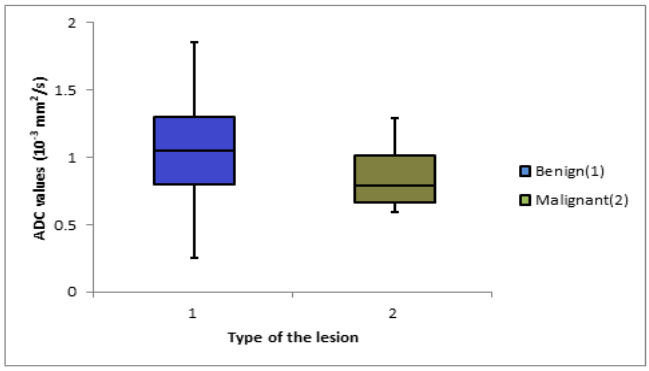

Fig. (7): Box plot graphs of apparent diffusion coefficient (ADC) values for benign and malignant lesions with range overlap.

Using b = 1000 s/mm^2, a receiver operator characteristic (ROC) curve was calculated. A cutoff point on the curve could distinguish benign and malignant tumors.

ADC values with a cutoff point of 1.0 × 10^{-3} mm^2/s or below could be considered for malignancy, with 66.67% sensitivity, 60% specificity, 62.5% positive predictive value, and 64.3% negative predictive value (Table 6 and Fig.8).

Table 6: ADCs sensitivity, specificity, positive and negative predictive values.

Cut off point	Sensitivity	Specificity	+PV	-PV	Like hood test
1.0	66.67 %	60.00 %	62.5 %	64.3 %	0.367

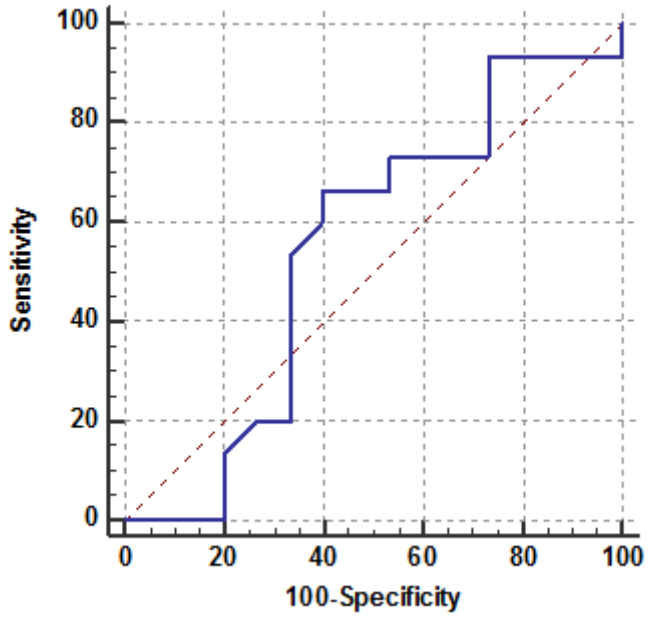

Fig. (8): Receiver operating characteristic (ROC) curve of ADC value in the studied group.

Discussion

Thyroid nodules are the most prevalent abnormality of the thyroid gland. Early detection of malignant nodules lowers disease mortality and morbidity rates. [7, 8]

Our goal was to assess the application of ADC values utilizing diffusion MRI with FNAC correlation in discriminating benign thyroid nodules from cancerous ones and identifying various pathological subtypes of each group.

Diffusion-weighted MRI Imaging (DWI) detects changes in tissue microstructure that affect water diffusion. A quantitative measure called the Apparent Diffusion Coefficient (ADC) can be used to identify if a thyroid nodule is malignant or benign. [9, 10]

Because they are significantly lower in malignant nodules, the ADC values can aid in distinguishing benign from malignant nodules. The ideal b value and the corresponding suggested cut-off point of ADC value to detect a malignant nodule are still up for debate. [11, 12]

In the current study we measures the mean ADC at b =1000, which is consistent with the findings of **Ravikanth et al.** [13], who noted that at higher b-values, there is a risk of noise contamination and poor image resolution, which leads to an unreliable ADC measurement; at lower b-values, there is a risk of perfusion contamination, which means the measured ADC will not be reliable to assess tissue diffusion due to mixed effects of perfusion and diffusion that could not be separated at these levels.

In this study, The mean ADC at b = 1000 was 1.02± 0.381 in benign lesions. Still, in malignant lesions, it was 0.73± 0.323 with a statistically significant difference between and P<0.001, which is in agreement with the study done by **Shokry et al.** [14], who reported that the ADC values in malignant group were significantly lower than in benign group (P value < 0.001), with benign group having a mean ADC value of 1.52 ± 0.35 and a range 0.7–2.2. The malignant group had a mean ADC value of 0.95 ± 0.29, ranging from 0.7 to 1.8.

In the current study, as regards the ROC curve, ADC revealed a 1.0 cut-off point, 66.67% sensitivity, 60% specificity, 62.5% positive predictive value, and 64.3% negative predictive value. On the other hand, the study conducted by **Noufal et al.** [15] had 94.4%, 96.8%, and 96.25% sensitivity, specificity, and accuracy, respectively. The outcomes align with the meta-analysis conducted by **Chen et al.** [16]

In their investigation, **Shokry et al.** [14] reported that the ADC measurement's cut-off value for distinguishing between both groups of nodules was 1.15, with 88.2% sensitivity and 92.3% specificity.

In the current study, the lymphocytic thyroiditis's ADC value varied between 1.31 and $2.60 \times 10^{-3} mm^2/s$. The ADC for colloid cysts and follicular adenomas varied from 1.0 to 2.5 $\times 10^{-3}$ mm^2/s and 0.66 to 2.37 $\times 10^{-3}$ mm^2/s, respectively. They were as follows: 0.21 – 0.96 ×

10^{-3} mm^2/s for follicular carcinoma; 0.51 – 1.0 × 10^{-3} mm^2/s for B-cell lymphoma; 0.22 – 1.30 × 10^{-3} mm^2/s for papillary carcinoma on top of follicular adenoma; 0.67 – 0.73 × 10^{-3} mm^2/s for medullary carcinoma; and 0.20 – 0.96 × 10^{-3} mm^2/s for papillary carcinoma.

In the current study, we could not distinguish between several pathological subtypes within each group separately, either benign or malignant group, utilizing the ADC value. The P value was 0.056 to 0.063.

The results of **Abdel Razek et al.** [17] found that the ADC values of the subtypes of the malignant group showed insignificant differences between them (P = 464), which were in line with this. Additionally, this was consistent with the findings of **Schueller-Weidekamm et al.** [18] (P = 0.058).

The complex composition of a benign thyroid nodule, which includes calcium, hemorrhage, fibrosis, minor necrosis, cystic alteration, and collagen, was thought to have an impact on the nodules' ADC values**.** However, this effect was not significant in differentiating between benign thyroid nodule subtypes. [12]

There are still some limitations in this study that affect the ability to differentiate between pathological subtypes of either benign or malignant nodules. The statistical power and analytical results are limited in some way by the relatively low percentage of certain pathological subtypes.

Conclusion and recommendation:

The distinction between benign and malignant groups can be made with the aid of diffusion-weighted MRI and ADC values, as they are much lower in malignant nodules. However, it is not possible to distinguish between the various pathological subtypes of either benign or malignant nodules.

Further research is needed to understand better the ADC's role in the area of early detection and differentiation between distinct pathological types with each benign or malignant groups of thyroid nodules.

Abbreviations

ADC: Apparent diffusion coefficient

EPI: Echo planner imaging

FNAC: Fine needle aspiration cytology

MRI: Magnetic resonance imaging

ROC: Receiver operating characteristics

ROI: Region of interest

SPSS: Statistical Package for the Social Sciences

STIR: Short tau inversion recovery

TE: Echo time

TR: Repetition time

US: Ultrasound

References

1. **Susana Calle, Jeanie Choi, Salmaan Ahmed, Diana Bell, &Kim O. Learned (2021).** Imaging of the thyroid. Neuroimaging Clinics. Volume 31, issue 3, P265-284.
2. **Araruna Bezerra de Melo, Fabio Menis, Vinicus Fernando Calsavara, Flavio Scavone Stefanini, Tullio Novaes & Mauro Saieg (2021).** The impact of the use of the ACR-TIRADS as a screening tool for thyroid nodules in a cancer center. Diagnostic Cytopathology, 50:18–23.
3. **Ehsan Seif, Mostafa Qorbani, Shaghayegh Mousavi, & Ali Salah Ashoor (2021).** A comparison of different Thyroid Imaging Reporting and Data Systems to reduce unnecessary FNAs and missed malignancies. Journal of Diagnostic Medical Sonography. Volume 38, Issue 2: 1–8.
4. **Kim, H.G., Moon, H.-J., Kwak, J.Y., Kim, E.-K.J.T., (2013).** Diagnostic accuracy of the ultrasonographic features for subcentimeter thyroid nodules suggested by the revised American Thyroid Association guidelines. 23, 1583-1589.
5. **Abdel-Rahman, H. M., Abo Warda, M. H., & Abdel-Aal, S. M. (2016).** Diffusion-weighted MRI and apparent diffusion coefficient in the differentiation of benign from the malignant solitary thyroid nodule. The Egyptian Journal of Radiology and Nuclear Medicine, 47(4), 1385-1390.
6. **Mohamad Nour M., Nael Ammaneh, Hussameddin Hasan Alali , & Fisal Haritani (2022).** Diagnosis and Pathology Characterization of Thyroid Gland Using

Different Radiological Techniques. European journal of molecular and clinical medicine. Volume 09. Issue 01.P284.

7. **Wang Q., Guo Y., Zhang J., Ning H., Zhang X., Lu Y., & Shi Q. (2019).** Diagnostic value of high b-value (2000 s/mm^2) DWI for thyroid micro-nodules. Medicine, 98(10). P e14298.
8. **Shi H. F., Feng, Q., Qiang J. W., Li R. K., Wang L., & Yu J. P. (2013).** Utility of diffusion-weighted imaging in differentiating malignant from benign thyroid nodules with magnetic resonance imaging and pathologic correlation. Journal of computer-assisted tomography, 37(4), 505-510.
9. **Noda, Y., Kanematsu, M., Goshima, S., Kondo, H., Watanabe, H., Kawada, H., & Bae, K. T. (2015).** MRI of the thyroid for differential diagnosis of benign thyroid nodules and papillary carcinomas. American Journal of Roentgenology, 204(3), W332-W335.
10. **Knox, M.A.J.A.F.P. (2013).** Thyroid nodules. Am Fam Physician. 1;88(3):193-6. PMID: 23939698.
11. **Nakahira, M., Saito, N., Murata, S.-i., Sugasawa, M., Shimamura, Y., Morita, K., Takajyo, F., Omura, G., Matsumura, S.J.A.j.o.o., (2012).** Quantitative diffusion-weighted magnetic resonance imaging as a powerful adjunct to fine needle aspiration cytology for assessment of thyroid nodules. 33, 408-416.
12. **Wu, Y., Yue, X., Shen, W., Du, Y., Yuan, Y., Tao, X., & Tang, C. Y. (2013).** Diagnostic value of diffusion-weighted MR imaging in thyroid disease: application in differentiating benign from malignant disease. BMC medical imaging, 13(1), 1-7.
13. **Ravikanth R, Selvam RP, & Pinto DS. (2017).** Role of quantitative diffusion-weighted magnetic resonance imaging in differentiating benign and malignant thyroid lesions. J Curr Res SciMed; 3:131-133.
14. **Shokry, A. M., Hassan, T. A., Baz, A. A., Ahmed, A. S. O., & Zedan, M. H. (2018).** Role of diffusion weighted magnetic resonance imaging in differentiation of benign and malignant thyroid nodules. The Egyptian Journal of Radiology and Nuclear Medicine, 49(4), 1014-1021.
15. **Noufal, P., Ramakrishnan, K., Kurup, S., Ali, N., Janardhanan, S., Rabia, T.A., Unni, V., Bernaitis, L.J.J.o.E.o.M., Sciences, D. (2018).** Differntiation between benign and malignant thyroid nodule with diffusion weighted magnetic resonance imaging and apparent diffusion coefficient measurment and its histopathological correlation. 7, 843-850.

16. **Chen, L., Xu, J., Bao, J., Huang, X., Hu, X., Xia, Y., Wang, J.J.B.o., (2016).** Diffusion-weighted MRI in differentiating malignant from benign thyroid nodules: a meta-analysis. 6, e008413.

17. **Abdel Razek AAK (2018)**. Routine and advanced diffusion imaging modules of the salivary glands. Neuroimag Clin; 28(2):245-254.

18. **Schueller-Weidekamm, C., Kaserer, K., Schueller, G., Scheuba, C., Ringl, H., Weber, M., Czerny, C., Herneth, A.J.A.j.o.n., (2009).** Can quantitative diffusion-weighted MR imaging differentiate benign and malignant cold thyroid nodules? Initial results in 25 patients. 30, 417-422.